Electronic supplementary information (ESI) for the manuscript:

Effective conversion of CO_2 into light olefins over bifunctional catalyst consisting of La-modified $ZnZrO_x$ oxide and acidic zeolite

Wenyu Zhang,[a,b] Sen Wang,*[,a] Shujia Guo,[a,b] Zhangfeng Qin,[a] Mei Dong,[a] Jianguo Wang,*[,a,b] and Weibin Fan,*[,a]

[a] *State Key Laboratory of Coal Conversion, Institute of Coal Chemistry, Chinese Academy of Sciences, P.O. Box 165, Taiyuan, Shanxi 030001, PR China*

[b] *University of the Chinese Academy of Sciences, Beijing 100049, PR China*

[*] *Corresponding authors. Tel.: +86-351-4046092; Fax: +86-351-4041153. E-mail address: wangsen@sxicc.ac.cn (S. Wang); iccjgw@sxicc.ac.cn (J. Wang); fanwb@sxicc.ac.cn (W. Fan)*

Table S1. Crystal structure and texture properties of various $ZnZrO_x$ and $ZnZrO_x$(*n*La) oxides. [a]

Catalysts	Phase	S_{BET} (m^2 g^{-1})	V_{mirco} (cm^3 g^{-1})	D_{size} (nm)	Cell volume (Å^3)
$ZnZrO_x$	Tetragonal	11.2	0.026	5.1(4.3)	66.17
$ZnZrO_x$(0.2La)	Tetragonal	100.2	0.106	2.6(3.5)	66.54
$ZnZrO_x$(0.3La)	Tetragonal	121.5	0.100	2.3(3.6)	66.69
$ZnZrO_x$(0.5La)	Amorphous	97.48	0.099	-	-
$ZnZrO_x$(1.0La)	Amorphous	71.8	0.067	-	-

[a] The phase structure and cell parameter of various samples were identified and calculated by the Rietveld refinement of XRD patterns. The surface area (S_{BET}) and pore volume (V_{mirco}) were obtained from N_2 sorption results by the BET and t-plot methods, respectively. The average particle sizes of NPs (D_{size}) were estimated by the Scherrer equation. The particle sizes in the parentheses were estimated by counting around 100 particles in the TEM images.

Figure S1.

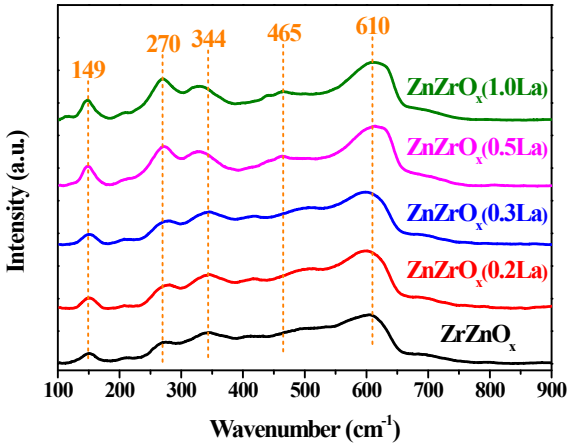

Figure S1. The Raman spectra of various $ZnZrO_x$ and $ZnZrO_x$(*n*La) oxides.

Figure S2.

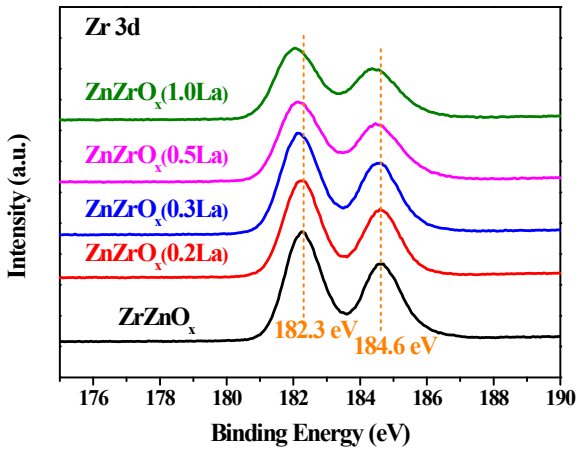

Figure S2. The Zr (3d) XPS of various $ZnZrO_x$ and $ZnZrO_x$(*n*La) oxides.

Figure S3.

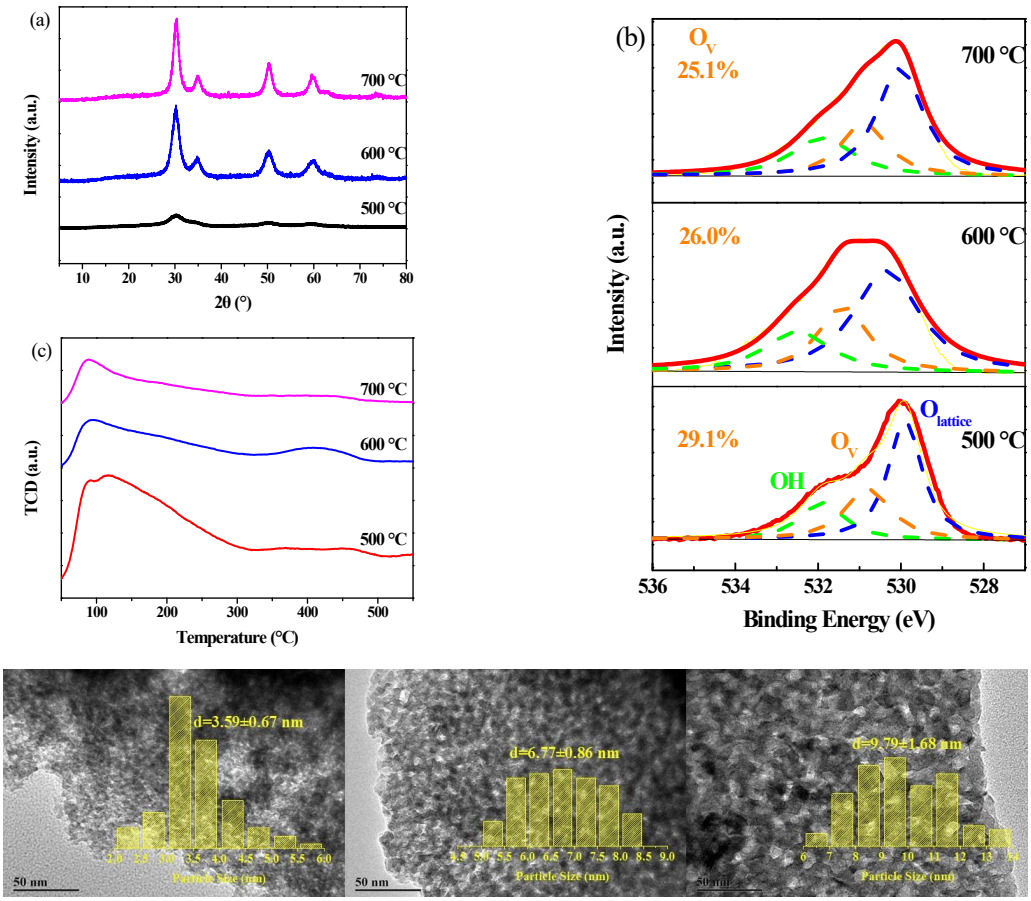

(d)

Figure S3. The XRD (a), O (1s) XPS (b), CO_2-TPD (c) and TEM images and the particle size distribution (estimated by counting around 100 particles) (d) of $ZnZrO_x$(0.3La) oxide calcinated at different temperatures.

Table S2. Crystal structure and texture properties of $ZnZrO_x$(0.3La) oxide prepared by using different calcinating temperatures. [a]

Catalysts	Phase	S_{BET} (m^2 g^{-1})	V_{mirco} (cm^3 g^{-1})	D_{size}(d) (nm)	Cell volume ($Å^3$)
$ZnZrO_x$(0.3La)-500℃	Tetragonal	121.5	0.100	2.3 (3.6)	66.69
$ZnZrO_x$(0.3La)-600℃	Tetragonal	38.1	0.042	4.3 (6.8)	67.54
$ZnZrO_x$(0.3La)-700℃	Tetragonal	26.9	0.060	6.0 (9.8)	68.03

[a] The phase structure and cell parameter of various samples were identified and calculated by the Rietveld refinement of XRD patterns. The surface area (S_{BET}) and pore volume (V_{mirco}) were obtained from N_2 sorption results by the BET and t-plot methods, respectively. The average particle sizes of NPs (D_{size}) were estimated by the Scherrer equation. The particle sizes in the parentheses were estimated by counting around 100 particles in the TEM images.

Figure S4.

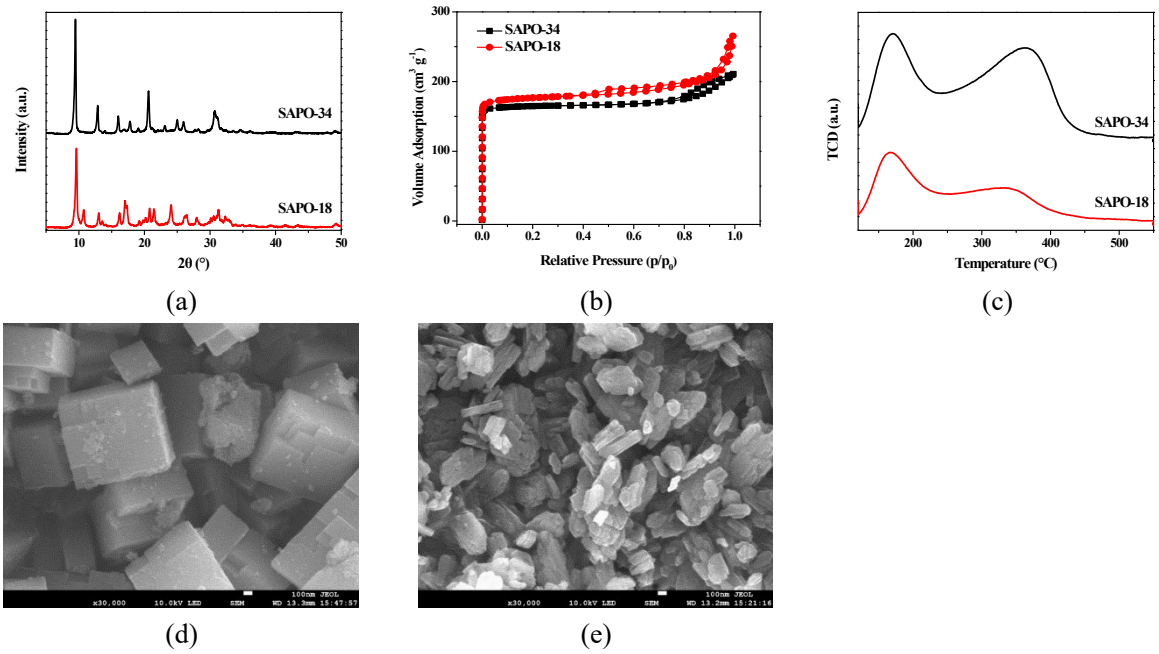

Figure S4. XRD patterns (a), N_2 sorption isotherm (b), NH_3-TPD profile (c) and SEM images (d for SAPO-34 and e for SAPO-18) of H-SAPO-34 and H-SAPO-18 zeolites.

Figure S5.

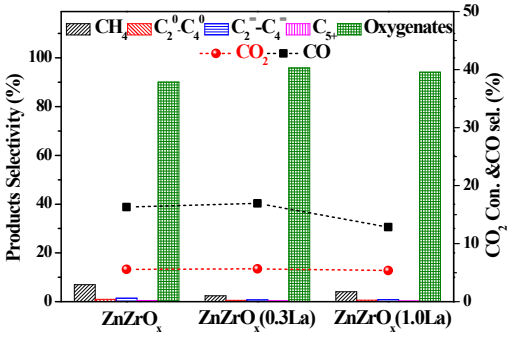

Figure S5. CO_2 conversion and product selectivity in CO_2 hydrogenation to methanol on various $ZnZrO_x$ and $ZnZrO_x$(*n*La) oxides at the same CO_2 conversion. Reaction conditions: 290-300 ºC, GHSV=4000-4800 mL g^{-1} h^{-1} and H_2/CO_2=3/1.

Figure S6.

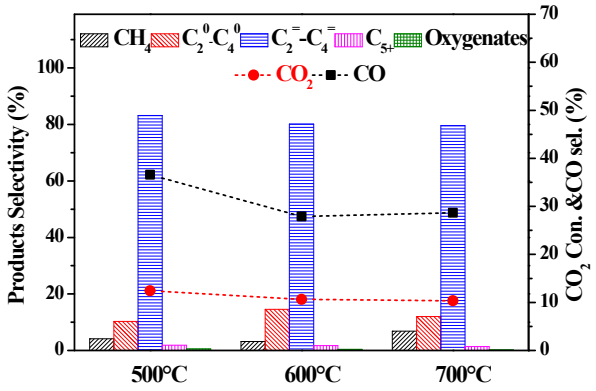

Figure S6. CO_2 conversion and product selectivity in CO_2 hydrogenation to light olefins on various $ZnZrO_x$(0.3La) oxides of different calcinating temperature. Reaction conditions: 350 ºC, 2.0MPa, GHSV=4000 mL g^{-1} h^{-1} and H_2/CO_2=3/1.

Figure S7.

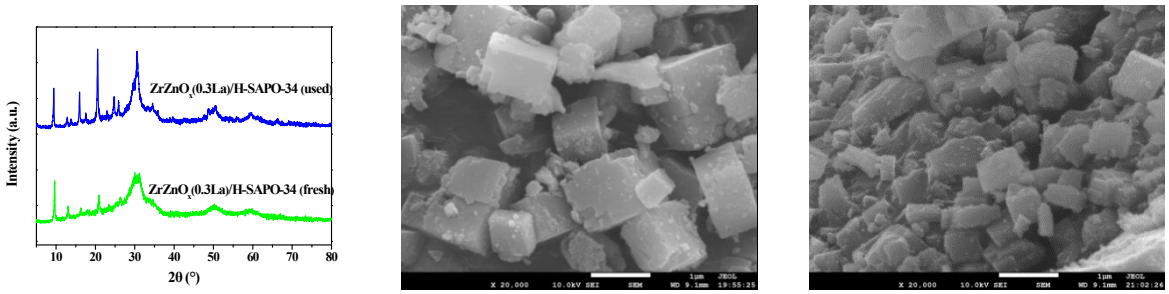

(a) (b) (c)

Figure S7. XRD patterns of fresh and used $ZnZrO_x$(0.3La)/H-SAPO-34 catalyst (a), SEM images of fresh (b) and used (c) $ZnZrO_x$(0.3La)/H-SAPO-34 catalyst.

Figure S8.

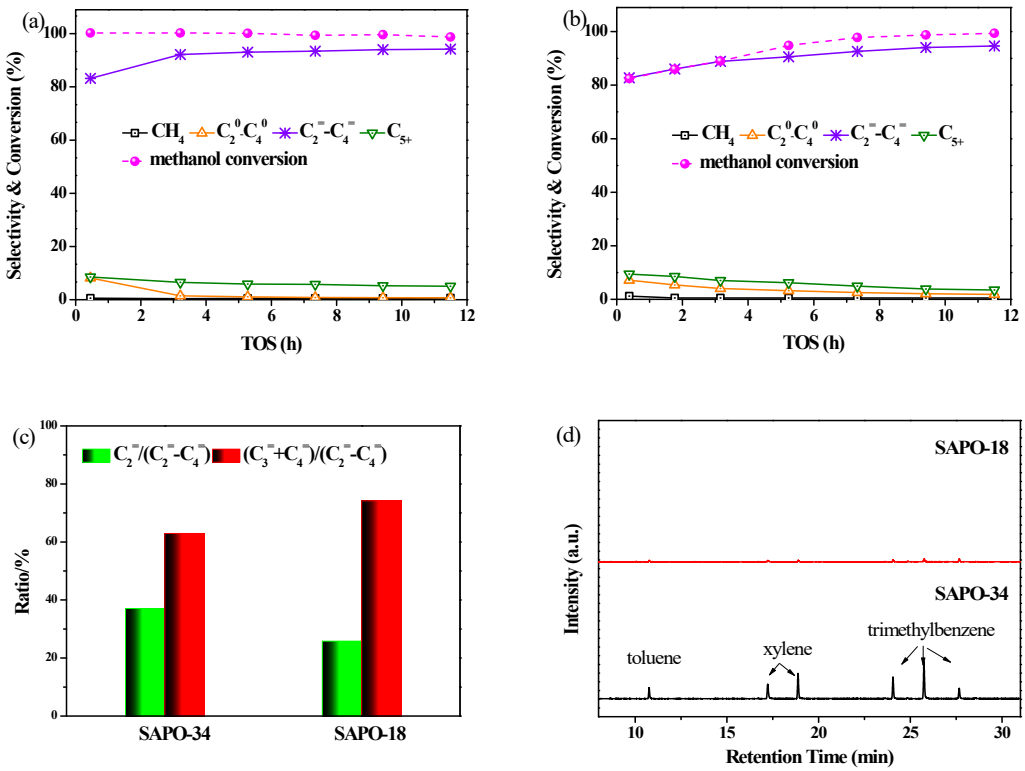

Figure S8. Methanol conversion and product selectivity in methanol to light olefins on H-SAPO-18 (a) and H-SAPO-34 (b) composite catalyst and the corresponding proportion of ethene and propene+butene in total $C_2^=$-$C_4^=$ (c), and GC-MS (d) of used H-SAPO-18 and H-SAPO-34. Reaction conditions: 350 ºC and $WHSV_{methanol}$ of 0.5 h^{-1}.

Figure S9.

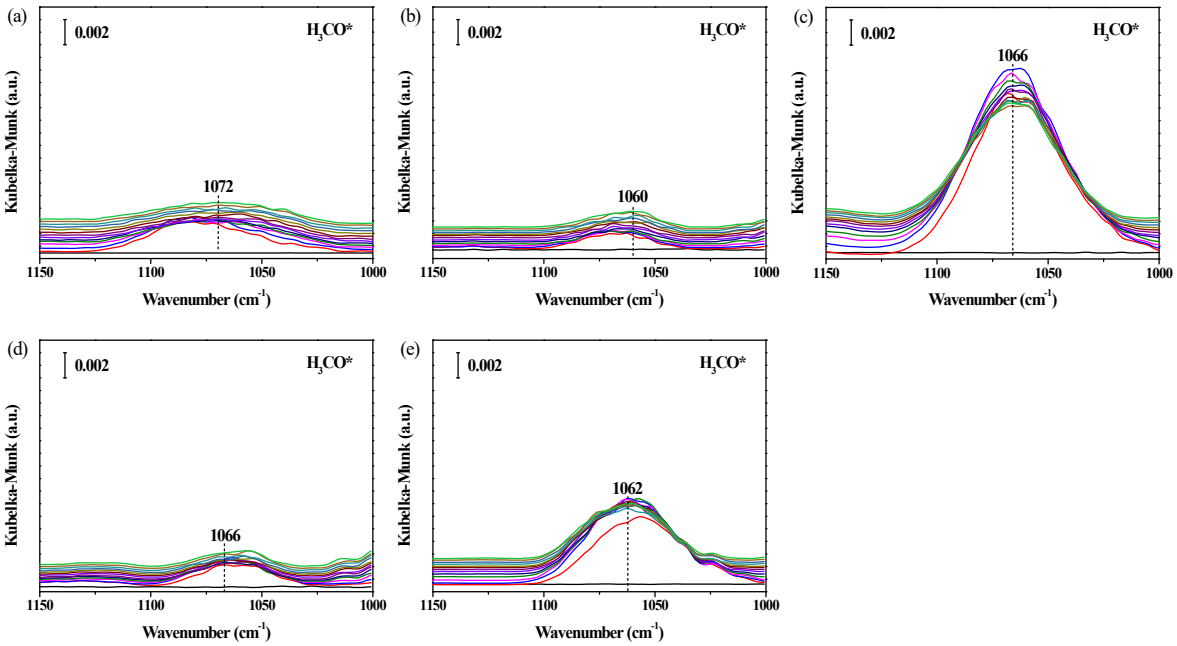

Figure S9. In situ DRIFTS in the range of 1000-1150 cm^{-1} for CO_2 hydrogenation on $ZnZrO_x$ (a), $ZnZrO_x$(0.2La) (b), $ZnZrO_x$(0.3La) (c), $ZnZrO_x$(0.5La) (d) and $ZnZrO_x$(1.0La) (e). The spectra was collected every 5 min up to 60 min after pre-treatment of the sample with H_2 (30 mL/min) for 2 h at 400 °C and purged with Ar (30 mL/min) for 0.5 h at 300 °C (Typical reaction conditions: 300 °C and 0.1 MPa).

Figure S10.

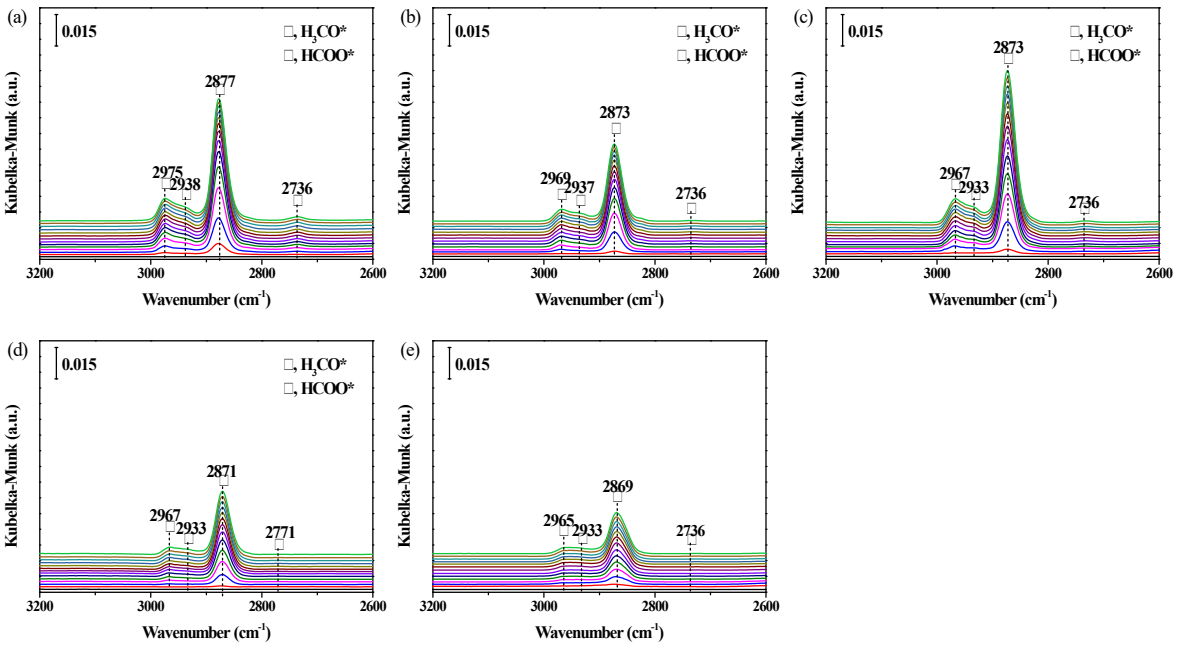

Figure S10. In situ DRIFTS in the range of 2600-3200 cm^{-1} for CO_2 hydrogenation on $ZnZrO_x$ (a), $ZnZrO_x$(0.2La) (b), $ZnZrO_x$(0.3La) (c), $ZnZrO_x$(0.5La) (d) and $ZnZrO_x$(1.0La) (e). The spectra was collected every 5 min up to 60 min after pre-treatment of the sample with H_2 (30 mL/min) for 2 h at 400 °C and purged with Ar (30 mL/min) for 0.5 h at 300 °C (Typical reaction conditions: 300 °C and 0.1 MPa).

Figure S11.

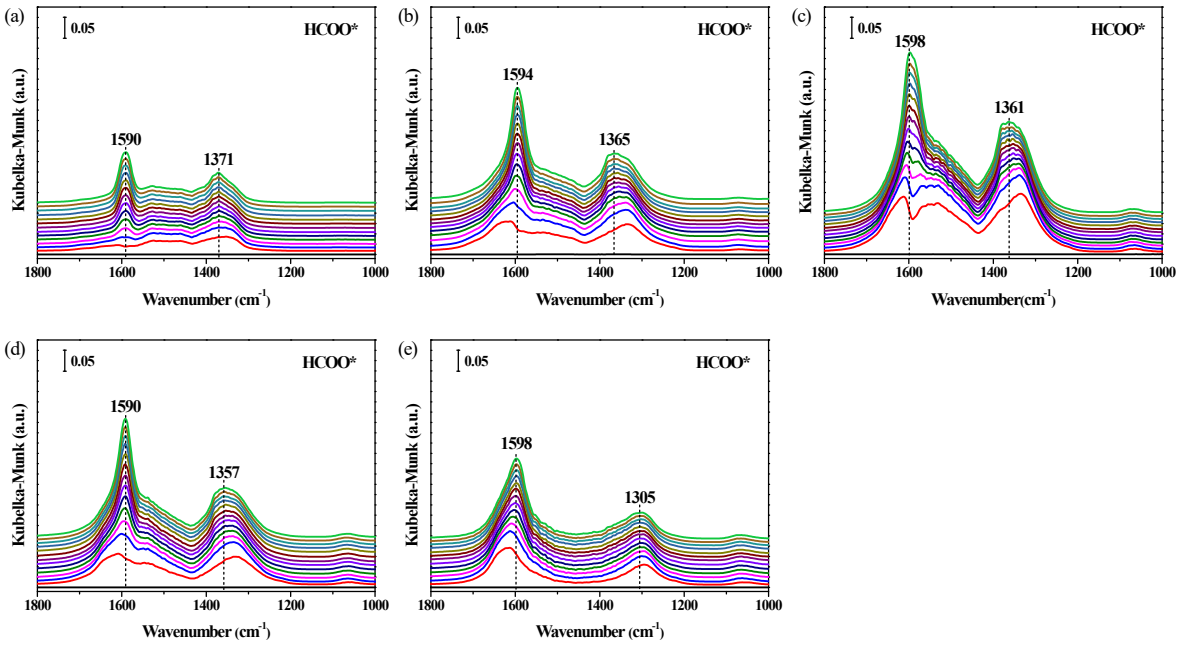

Figure S11. In situ DRIFTS for CO_2 hydrogenation on $ZnZrO_x$ (a), $ZnZrO_x$(0.2La) (b), $ZnZrO_x$(0.3La) (c), $ZnZrO_x$(0.5La) (d) and $ZnZrO_x$(1.0La) (e). The spectra was collected every 5 min up to 60 min after pre-treatment of the sample with H_2 (30 mL/min) for 2 h at 400 °C and purged with Ar (30 mL/min) for 0.5 h at 260 °C (Typical reaction conditions: 260 °C and 0.1 MPa).

Figure S12.

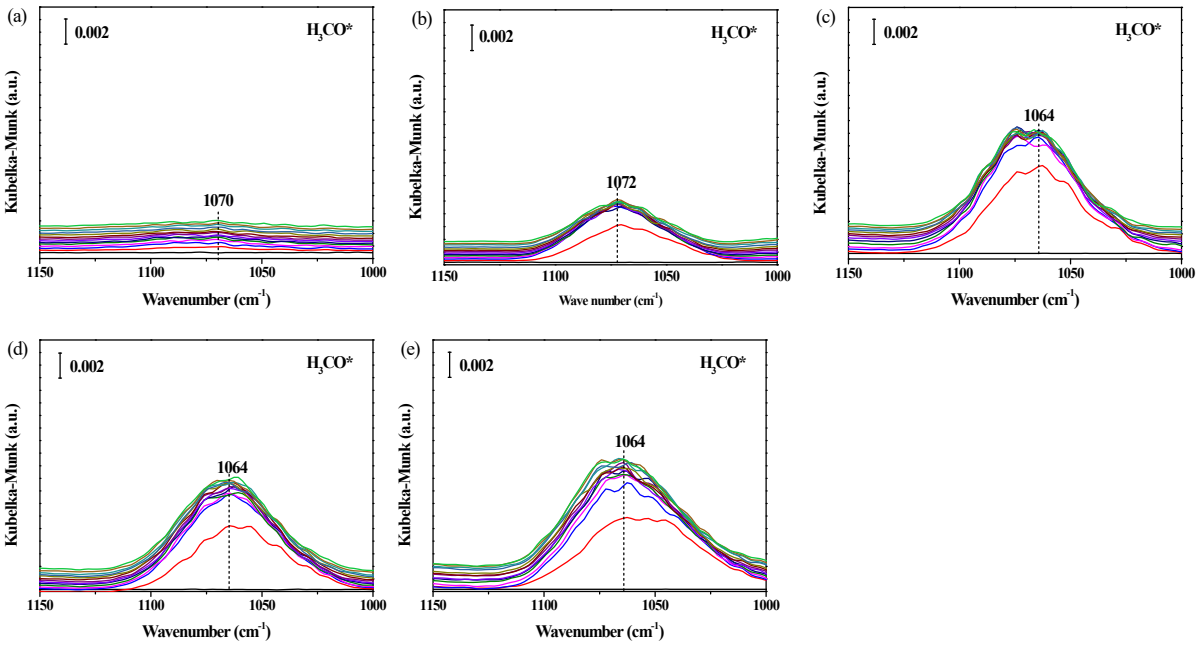

Figure S12. In situ DRIFTS in the range of 1000-1150 cm^{-1} for CO_2 hydrogenation on $ZnZrO_x$ (a), $ZnZrO_x$(0.2La) (b), $ZnZrO_x$(0.3La) (c), $ZnZrO_x$(0.5La) (d) and $ZnZrO_x$(1.0La) (e). The spectra was collected every 5 min up to 60 min after pre-treatment of the sample with H_2 (30 mL/min) for 2 h at 400 °C and purged with Ar (30 mL/min) for 0.5 h at 260 °C (Typical reaction conditions: 260 °C and 0.1 MPa).

Figure S13.

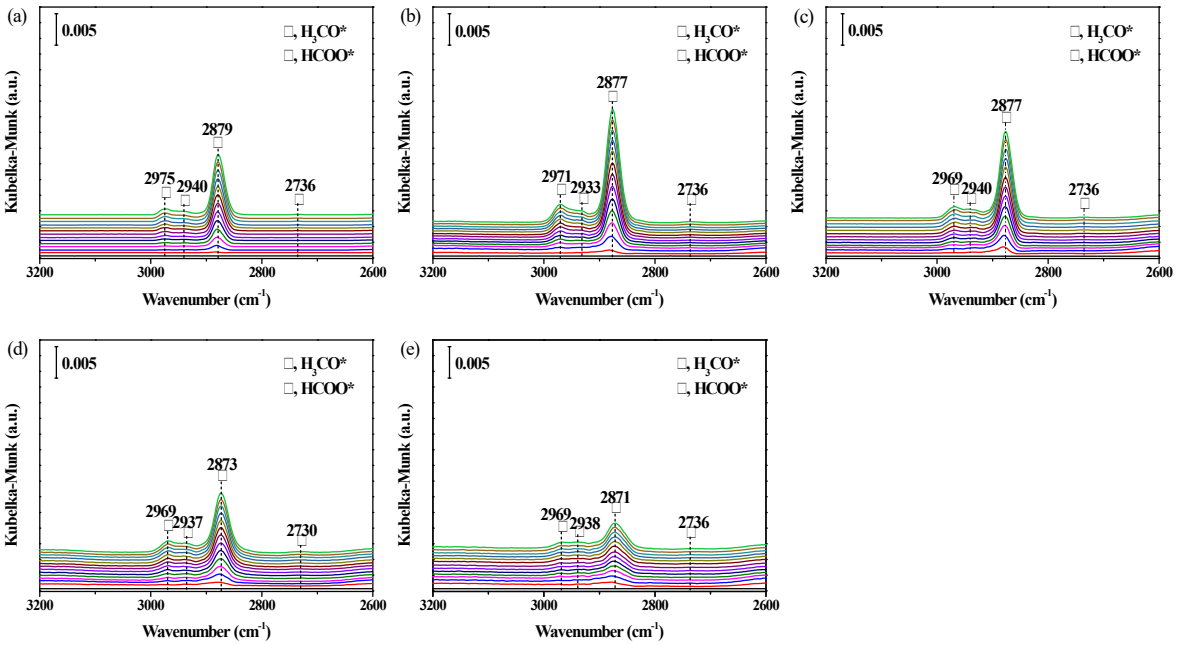

Figure S13. In situ DRIFTS in the range of 2600-3200 cm^{-1} for CO_2 hydrogenation on $ZnZrO_x$ (a), $ZnZrO_x$(0.2La) (b), $ZnZrO_x$(0.3La) (c), $ZnZrO_x$(0.5La) (d) and $ZnZrO_x$(1.0La) (e). The spectra was collected every 5 min up to 60 min after pre-treatment of the sample with H_2 (30 mL/min) for 2 h at 400 °C and purged with Ar (30 mL/min) for 0.5 h at 260 °C (Typical reaction conditions: 260 °C and 0.1 MPa).

Figure S14.

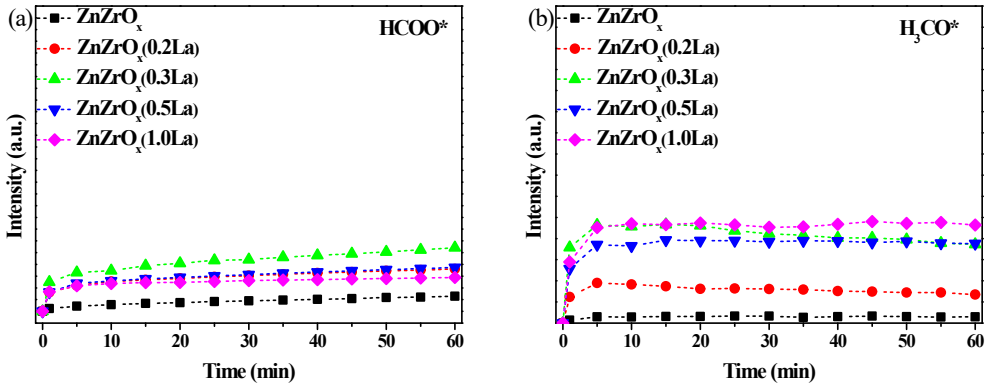

Figure S14. Variation of peak intensity of formate (a) and methoxy (b) intermediates with the reaction time over various $ZnZrO_x$ and $ZnZrO_x$(*n*La) oxides (Typical reaction conditions: 260 °C and 0.1 MPa).

Figure S15.

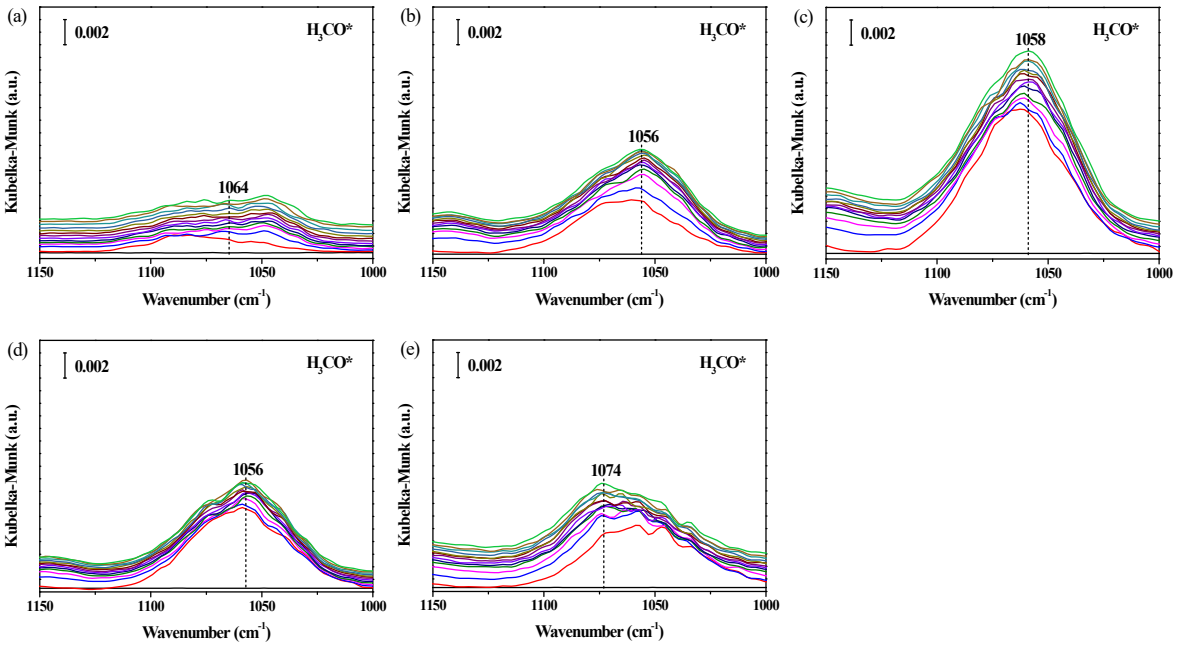

Figure S15. In situ DRIFTS in the range of 1000-1150 cm^{-1} for CO_2 hydrogenation on $ZnZrO_x$ (a), $ZnZrO_x$(0.2La) (b), $ZnZrO_x$(0.3La) (c), $ZnZrO_x$(0.5La) (d) and $ZnZrO_x$(1.0La) (e). The spectra was collected every 5 min up to 60 min after pre-treatment of the sample with H_2 (30 mL/min) for 2 h at 400 °C and purged with Ar (30 mL/min) for 0.5 h at 350 °C (Typical reaction conditions: 350 °C and 0.1 MPa).

Figure S16.

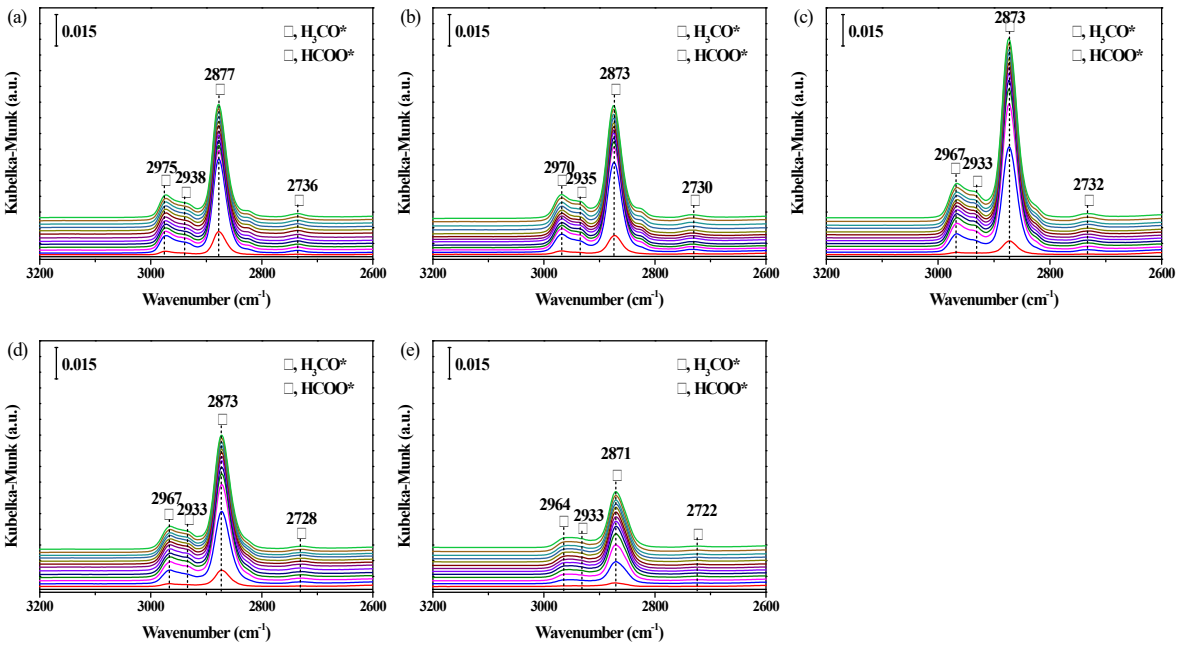

Figure S16. In situ DRIFTS in the range of 2600-3200 cm^{-1} for CO_2 hydrogenation on $ZnZrO_x$ (a), $ZnZrO_x$(0.2La) (b), $ZnZrO_x$(0.3La) (c), $ZnZrO_x$(0.5La) (d) and $ZnZrO_x$(1.0La) (e). The spectra was collected every 5 min up to 60 min after pre-treatment of the sample with H_2 (30 mL/min) for 2 h at 400 °C and purged with Ar (30 mL/min) for 0.5 h at 350 °C (Typical reaction conditions: 350 °C and 0.1 MPa).

Figure S17.

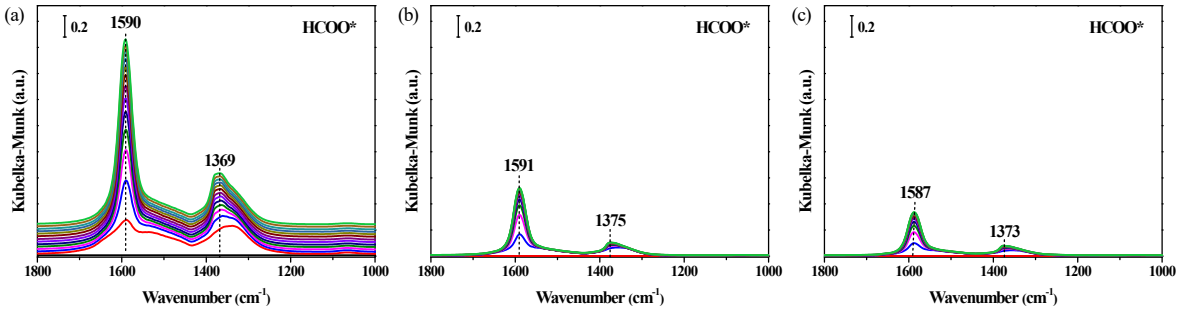

Figure S17. In situ DRIFTS for CO_2 hydrogenation on $ZnZrO_x$(0.3La)-500 °C (a), $ZnZrO_x$(0.3La)-600 °C (b) and $ZnZrO_x$(0.3La)-700 °C (c). The spectra was collected every 1 min up to 15 min after pre-treatment of the sample with H_2 (30 mL/min) for 2 h at 400 °C and purged with Ar (30 mL/min) for 0.5 h at 300 °C (Typical reaction conditions: 300 °C and 0.1 MPa).

Figure S18.

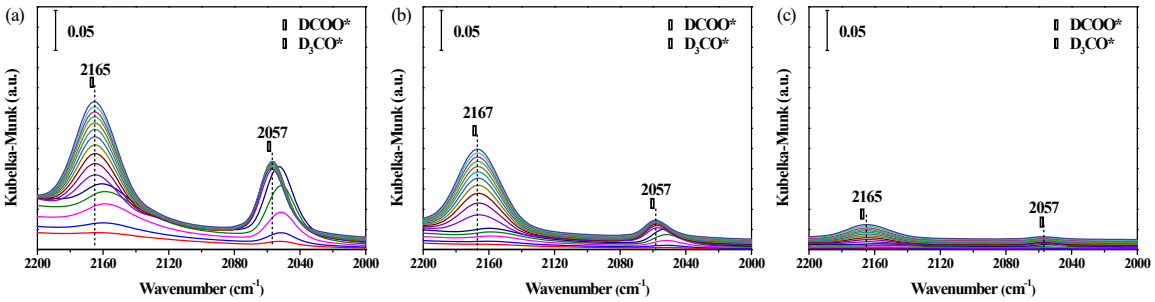

Figure S18. Isotope-labeled in situ DRIFTS for CO_2 hydrogenation on $ZnZrO_x$(0.3La)-500 °C (a), $ZnZrO_x$(0.3La)-600 °C (b) and $ZnZrO_x$(0.3La)-700 °C (c). The spectra was collected every 1 min up to 15 min after pre-treatment of the sample with H_2 (30 mL/min) for 2 h at 400 °C and purged with Ar (30 mL/min) for 0.5 h at 300 °C (Typical reaction conditions: 300 °C and 0.1 MPa).

Table S3. The catalytic performance of previous reported bifunctional catalysts in CO_2 hydrogenation to light olefins.

Catalysts	T/K	P/MPa	CO_2 Conv./%	$C_2^=$-$C_4^=$ Sel./%	CO Sel./%	$C_2^=$-$C_4^=$ Yield/%	Refs.
Zr-In_2O_3 /SAPO-34	673	3	35.5	76.4	85.0	4.1	[1]
ZnO-ZrO_2 /SAPO-34	653	3	12.6	80.0	43.0	5.7	[2]
$ZnAl_2O_4$ /SAPO-34	643	3	15	87.0	49.0	6.6	[3]
$ZnGa_2O_4$ /SAPO-34	643	3	13.0	86.0	46.0	6.0	[4]
$ZnZrO_x$ (0.3La)/SAPO-34	623	2	12.4	83.2	36.5	6.6	This work
$ZnZrO_x$ (0.3La)/SAPO-18	623	2	11.9	77.5	31.6	6.3	This work

[1] P. Gao, S. S. Dang, S. G. Li, X. N. Bu, Z. Y. Liu, M. H. Qiu, C. G. Yang, H. Wang, L. S. Zhong, Y. Han, Q. Liu, W. Wei and Y. H. Sun, *Acs Catalysis*, 2018, **8**, 571-578.

[2] Z. L. Li, J. J. Wang, Y. Z. Qu, H. L. Liu, C. Z. Tang, S. Miao, Z. C. Feng, H. Y. An and C. Li, *Acs Catalysis*, 2017, **7**, 8544-8548.

[3] X. L. Liu, M. H. Wang, H. R. Yin, J. T. Hu, K. Cheng, J. C. Kang, Q. H. Zhang and Y. Wang, *Acs Catalysis*, 2020, **10**, 8303-8314.

[4] X. L. Liu, M. H. Wang, C. Zhou, W. Zhou, K. Cheng, J. C. Kang, Q. H. Zhang, W. P. Deng and Y. Wang, *Chemical Communications*, 2018, **54**, 140-143.